Published in final edited form as:
Bioconjug Chem. 2009 March 18; 20(3): 583–590. doi:10.1021/bc8005094.

Design, synthesis and preliminary *in vitro* and *in vivo* evaluation of 4-[^{18}F]fluoro-*N*-(2-diethylaminoethyl)benzamide ([^{18}F]-DAFBA): A novel potential PET probe to image melanoma tumors

Sudha Garg, **Kanchan Kothari**, **Shankar R. Thopate**, **Aniruddha K. Doke**, and **Pradeep K. Garg***
PET Center, Department of Radiological Sciences, Wake Forest University Medical Center, Winston Salem, NC

Abstract

In order to develop a PET radiopharmaceutical to image malignant melanoma, we synthesized *N*-(2-diethylaminoethyl)-4-[^{18}F]fluorobenzamide ([^{18}F]-DAFBA). *In vitro* studies show a high uptake of [^{18}F]-DAFBA by the B16F1 melanoma cells. No significant binding was seen for DAFBA to the sigma-1 and sigma-2 receptors *in vitro*. The i*n vivo* biodistribution studies performed in normal ICR mice showed a low uptake in the normal tissues followed by further elimination of radioactivity from these tissues with time. The biodistribution studies performed in C57 mice bearing melanoma tumor xenograft showed a rapid uptake of radioactivity in the tumor that reached a plateau within 30 min post injection. The F-18 uptake in the tumor was 7.00±2.76, 6.57±1.66, and 5.80±0.98 %ID/g at 60, 120, and 180 min, respectively. A steady uptake of radioactivity in the tumor and low uptake in normal tissues resulted in high tumor to normal tissue ratios. For example, at 180 min post-injection, the tumor to tissue ratios were 14.90±6.47, 21.90±4.68, 32.91±6.11, 36.73±5.61, and 6.33±1.9, for the spleen, lungs, muscle, blood, and liver, respectively. The radioactivity rapidly cleared from the blood pool and it decrease from 0.58±0.18 %ID/g at 60 min to 0.13±0.03 %ID/g at 180 min. The F-18 uptake in the bones at 60, 120, and 180 min was 0.91±0.27, 0.57±0.32, and 0.17±0.05 %ID/g, respectively. This low uptake in the bones reflects its *in vivo* resistance towards de-fluorination. A low residual activity in normal tissues and a high tumor uptake signifies a superior imaging potential of this compound. Owing to these positive traits, [^{18}F]-DAFBA could help delineate tumor and its metastases when used for imaging application. Further *in vivo* studies are underway to assess potential of [^{18}F]-DAFBA as a promising PET imaging probe.

Keywords

Melanoma Imaging agent; *N*-(2-diethylaminoethyl)-4-[^{18}F]fluorobenzamide; Positron Emission Tomography (PET); F-18 fluorobenzamide; DAFBA; biodistribution studies; melanoma tumor xenograft; *in vitro* cell uptake; tumor uptake

INTRODUCTION

Skin cancer is one of the most common cancers in the USA and one in five people will develop it over the course of their lives. While melanoma accounts for only 3% of all skin cancer cases, 75% of deaths in this group are associated with melanoma. Unfortunately, incidence of melanoma is increasing more rapidly than any other cancer. The patient prognosis and their

*Author for Correspondence: Pradeep K. Garg, PET Center, Department of Radiological Sciences, Wake Forest University Health Sciences, Winston Salem, NC 27157, 336-716-5624, 336-716-5639 (FAX), pgarg@wfubmc.edu.

survival heavily depend on clinical stage of the disease at the time of diagnosis. For example, a ten year survival rate for stage 1 melanoma patients is 90–97% and only 3% for stage IV melanoma patients. Therefore, an early diagnosis of this disease and accurate assessment of its metastases remains the key for improved outcome and disease free survival. Several scintigraphic probes such as monoclonal antibodies to melanoma associated antigens (1,2), peptides (3,4), amino acids (5), iodoquinolines (5,6), iodoamphetamine (7,8), and guanidines (9) have been developed over the years to detect melanoma and localize metastatic lesions. While some of these compounds showed their potential in preliminary evaluations, none of these agents could achieve clinical significance. Therefore, the goal of many research groups including ours has been to develop diagnostic imaging agents with higher specificity and sensitivity to melanoma. More recently, a series of iodinated benzamides were synthesized as potential melanoma imaging agents. Because of the high affinity of iodobenzamides towards melanocytes and favorable tissue distribution characteristics, some of these radioiodinated benzamides were further pursued in humans to image melanoma tumors. This concerted effort yielded several clinically useful scintigraphic probes with good imaging characteristics (10–13). For an effective treatment outcome, it is important to accurately localize the tumor and its micrometastatic lesions. While positron emission tomography (PET) has recently emerged as an effective and non invasive 3-D tomographic imaging modality to provide absolute quantitative data on tracer uptake in the tissues, efforts to develop a PET probe to image melanoma have been rather sparse. The advantages of PET imaging include its ability to provide absolute quantitative data, ease in background subtraction, and tomographic imaging. At present, F-18 FDG PET imaging remains the only available imaging probe to localize melanoma cancer, despite its inherent drawbacks. For example, it is difficult to detect smaller tumor volumes using FDG (14). In addition, the sensitivity of these scans depends largely on the stage of the disease. FDG PET sensitivity to detect stage 1 melanoma is 0% but improves to 81% for stage III (15), thus ruling out its utility in early detection of melanoma. In previous studies, the FDG failed to detect metastatic disease in all patients with positive sentinel node biopsy (16). Presence of infection, inflammation, or recent surgery further increases the rate of false positive results, thus diminishing its efficacy as a reliable diagnostic tool (17). F-18 FDG lacking specificity towards melanoma underscores the need to search for more effective probes for early detection of melanoma cancer.

Since *N*-diethylaminoethyl 4-[*I]iodobenzamide (4-[*I]BZA) and *N*-diethylaminoethyl 2-[*I] iodobenzamide (2-[*I]IBZA) showed clinical potential and is being used in the clinics to image melanoma (10,18–21), it was imperative that we focus our initial efforts to develop a PET analogue using the same structural motif. Towards that goal, we replaced the 4-iodo group of 4-[*I]IBZA with a 4-fluoro group while keeping the remainder of the molecule unchanged. If successfully synthesized and promising biological characteristics are observed, this new PET probe could be a useful technique for early detection of melanoma, especially when lesions are small in size and difficult to detect. In order to develop this PET probe, we initially synthesized the non radioactive compound *N*-(2-diethylaminoethyl) 4-fluorobenzamide (DAFBA, **1**). This compound was synthesized using a one step synthesis procedure. The radiochemistry to incorporated F-18, a PET radioisotope to prepare *N*-(2-diethylaminoethyl) 4-[^{18}F]fluorobenzamide ([^{18}F]-DAFBA) was accomplished using a three step synthesis. Herein, we describe our results from the synthesis of [^{18}F]-DAFBA, the *in vitro* uptake to melanoma cells, and its *in vivo* distribution characteristics in normal mice and in mice with a melanoma tumor xenograft.

EXPERIMENTAL PROCEDURES

All reactions were carried out under an inert argon atmosphere using dry solvents under anhydrous conditions, unless otherwise stated. Reagents and solvents were purchased from commercial suppliers and were used without further purification. The C-18 plus Sep-Pack and

the QMA cartridges were obtained from Waters Corporation, USA. Melting points were determined on an Electrothermal "MEL-TEMP" melting point apparatus and are uncorrected. Flash column chromatography was carried out over silica gel (60 Å, Mallinckrodt, Baker). ^{1}H NMR data was acquired on a Bruker Advance 300 DPX spectrometer. All chemical shift values are reported in ppm (δ).

High performance liquid chromatography (HPLC) was performed in isocratic mode using a Varian 9010 LC pump, a variable wavelength 9050UV VIS detector (Varian Corp, Palo Alto, CA, USA) set at 254 λ, and a radioisotope detector (Bioscan Inc, Washington DC, USA) attached to Varian's chromatography software package. The radiochemical yields reported are decay corrected and are calculated to end of bombardment (EOB) time. The HPLC system used for the purification of [^{18}F]-DAFBA was a C-18 reverse-phase, 7.5×250 mm 5μ column (Phenomenex, Torrence, CA) eluted with MeOH:0.1M ammonium formate (30:70) using a flow rate of 3 mL/min. Quality control of purified product was carried out on C-18 QC column (4.6mm × 250mm, 5 μm) eluted with methanol:0.1M ammonium acetate (50:50) solvent system containing 40 μL of triethyl amine/100 mL of solvent with a flow rate of 1mL/min. The kryptofix solution was prepared by dissolving 120 mg of K222 and 720 mg of K_2CO_3 in 720 μL water followed by adding 12 mL of acetonitrile. The C-18 Sep-Pak cartridge was activated by passing 5 mL of ethanol followed by 5 mL of sterile water. The QMA cartridge was activated by washing the cartridge with 5 mL of 1N sodium bicarbonate solution followed by flushing it with 10 mL of water and then drying it by passing air through the cartridge for ~30 sec.

The melanoma cells (B16F1) were purchased from American Type Culture Collection (ATCC, Rockville, MD) and were grown in Dulbecco's Modified Eagle's Medium (DMEM) supplemented with 10% fetal bovine serum at 37°C in an incubator maintaining a 5% CO_2 environment. The ICR and the C57 mice (6–8 weeks old) were purchased from the Charles River Laboratories. Animal studies were performed under the guidelines established by the Wake Forest University Institutional Animal Care and Use Committee. The radioactivity levels in tissues were assessed with a Packard Cobra γ-counter.

Chemistry

Preparation of N-(2-diethylaminoethyl)-4-fluorobenzamide (DAFBA, 1)—This compound was synthesized as shown in Scheme 1. A solution of 4-fluorobenzoic acid (1.42 gm, 10.3 mmol) in 50 mL dichloromethane was cooled to 0°C using an ice bath. To this ice cooled solution, triethylamine (1.3 g, 12.9 mmol) and ethyl chloroformate (1.2 g, 11.1 mmol) were added and the reaction mixture was stirred for 1 hr at 0°C. A solution of N,N-diethylethylenediamine (1.0 g, 8.6 mmol) in dichloromethane (10 mL) was added slowly to this reaction mixture. After the addition was completed, the flask was removed from the ice bath and the reaction mixture was stirred for 2 hr at room temperature. Subsequently, the reaction mixture was cooled in the ice bath and the reaction was quenched with 10 mL of 3N NaOH. The product was extracted from crude reaction mixture using dichloromethane (2 × 30 mL). The combined organic layer was dried over sodium sulfate. After evaporating the solvent, a light-yellow colored oil was obtained that was further purified using flash column chromatography (acetone). The desired product 1 was collected as colorless viscous oil (1.96 g, 96% yield). ^{1}H NMR ($CDCl_3$, δ): 1.04 (t, 6H, *J*= 7.2 Hz, 2 × –CH_2-C**H**$_3$), 2.56 (q, 4H, *J*= 7.2 Hz, 2 x –C**H**$_2$-CH_3), 2.64 (t, 2H, *J*= 6.3 Hz, -C**H**$_2$-N–(CH_2-CH_3)$_2$), 3.44 – 3.49 (m, 2H, -CONH-C**H**$_2$-), 6.87 (br S, 1H, -N**H**), 7.07 – 7.14 (m, 2H, Ar-H @ C3 and C5), 7.75 – 7.81 (m, 2H, Ar-H @ C2 and C6).

Ethyl-4-(N,N,N-trimethylammonium trifluoromethanesulfonyl)benzoate (2)—This compound was prepared as a precursor for the radiofluorination reaction by using a method

analogous to that reported earlier with minor modifications (22–24). Briefly, ethyl 4-(dimethylamino) benzoate (0.5 g) was dissolved in dichloromethane (20 mL) and the solution was cooled in an ice bath. To this ice cold solution, methyl trifluoromethanesulfonate (0.5 mL) was slowly added while stirring. After the addition was completed, the reaction mixture was stirred for an additional 30 min, filtered, and a colorless to whitish crystalline product was collected as the target compound (0.84 g) mp 110–112°C (Lit mp 112–114°C (24)). 1H NMR ($CDCl_3$, δ): 1.37 (t, 3H, *J*= 7.2Hz, -$OCH_2\mathbf{CH_3}$), 3.66 (s, 9H, -$N(\mathbf{CH_3})_3$), 4.40 (q, 2H, *J*= 7.2Hz, -$O\mathbf{CH_2}CH_3$), 7.94 (d, 2H, *J*= 9.3Hz, Ar-H close to $N(Me_3)_3$), 8.21 (d, 2H, *J*= 9.3Hz, Ar-H close to -COOEt).

Radiochemical Synthesis of N-[2-(diethylamino)ethyl]-4-[^{18}F]fluorobenzamide ([^{18}F]-DAFBA)—The radiochemical synthesis of [^{18}F]-DAFBA was accomplished by first synthesizing 4-[^{18}F]fluorobenzoic acid followed by its coupling to N,N-diethylethylenediamine, using 1-(3-dimethylaminopropyl)-3-ethylcarbodiimide hydrochloride (EDC) as the coupling agent. The radiochemical synthesis of this compound is shown in Scheme 2.

Synthesis of 4-[^{18}F]fluorobenzoic acid (4)—Aqueous [^{18}F]fluoride was produced by using an $^{18}O(p, n)^{18}F$ reaction on 95% enriched [^{18}O]-H_2O in a high volume, high pressure [^{18}F]fluoride target irradiated with a 45μA beam current. After the irradiation, the ^{18}O-H_2O bolus containing 450 – 800 mCi of [^{18}F]-fluoride was transferred from the cyclotron onto an AG1X8 (Bio-Rad) anion exchange resin cartridge in the hot-cell and the [^{18}O]-H_2O was recovered. The trapped [^{18}F]fluoride was eluted from the cartridge with aqueous Cs_2CO_3 (0.3ml, 1mM) into a reaction vessel. The remainder of water from this mixture was removed azeotropically using acetonitrile. The dried [^{18}F]fluoride was resolubilized in 10μL aqueous Cs_2CO_3 solution (1mM) and reacted with 4-formyl N,N,N-trimethylbenzeneaminium trifluoromethane sulfonate dissolved in 120μL DMSO, following the procedure described earlier (24). The 4-[^{18}F]fluorobenzaldehyde (**2**) thus obtained was oxidized by reacting with a 5% solution of KMnO4 in 1N NaOH (300 μL) at 120°C for 10 min. Subsequently, sodium bisulphate solution (150 μg in 300 μL water) and 5N HCl (0.5mL) were added. The contents were diluted with 6 mL of water, passed through a C-18 Sep-Pak cartridge, rinsed with 10 mL of water, and the 4-[^{18}F] fluorobenzoic acid (**4**) was eluted from the cartridge in 72 ± 11% (n=12) radiochemical yields with 3 mL of acetonitrile.

Alternate synthesis of 4-[^{18}F]fluorobenzoic acid via the ethyl-4-[^{18}F] fluorobenzoate as an intermediate—After the irradiation, the ^{18}O-H_2O bolus containing 450 – 800 mCi of [^{18}F]-fluoride was transferred from the cyclotron onto a pre-activated QMA cartridge in the hot-cell and the [^{18}O]-H_2O was recovered. The trapped [^{18}F]fluoride was eluted from the cartridge with 1.5 mL of K2.2.2. solution prepared as described above. The remainder of water from this mixture was removed azeotropically using acetonitrile. The dried [^{18}F] fluoride was reacted with a freshly prepared solution of 5 mg of precursor ethyl-4-(trimethylammonium triflate)benzoate in 120 μL of anhydrous DMSO at 106°C for 10 min as described earlier (25). Subsequently, the reaction vessel was cooled to room temperature, 500 μL of 1N NaOH was added, and the reaction mixture was heated for 5 min at 100°C to hydrolyze the ester group without isolating the intermediate 3. After cooling the reaction mixture to room temperature, the contents were acidified using 1N HCl (~600 μL), and loaded onto a C-18 Sep-Pak cartridge for purification. The Sep-Pak was washed with 10 ml of water and 4-[^{18}F] fluorobenzoic acid (**4**) was eluted from the cartridge using 3.5 mL of acetonitrile.

Coupling of 4-[^{18}F]fluorobenzoic acid with N-N diethylethylenediamine to prepare [^{18}F]-DAFBA—The solvent from 4-[^{18}F]fluorobenzoic acid solution (**4**) obtained using either of the above two methods was reduced to ~300 μL. (Note: evaporating to lesser

volume resulted in loss of radioactivity). A solution of 1-hydroxybenzotriazole hydrate (HOBT, 3 mg) in 100 μL DMF, 1-(3-dimethylaminopropyl)-3-ethylcarbodiimide hydrochloride (EDC, 3.5 mg), and *N*-*N*-diethylethylenediamine (1 mg) in DMF (100 μL) were added sequentially to the reaction vessel containing 4-[^{18}F]fluorobenzoic acid and the reaction mixture was stirred for 30 min at room temperature. The solvent was evaporated to ~150 μL using a gentle stream of nitrogen, diluted with 1mL HPLC mobile phase and the contents were loaded onto the HPLC column to isolate the desired product. The desired product collected from HPLC and the solvent was evaporated using a rotary evaporator. The residue was re-dissolved in 0.5 L ethanol and 9.5 mL of water was added. The product solution was then filtered through a 0.22 μ filtering cartridge and collected in a 20 mL sterile product vial.

Stability Measurement—A solution of [^{18}F]-DAFBA (5 mCi) in 2 mL saline was assayed for its room temperature shelf-life stability using the HPLC method. An aliquot (100 μL) of the above solution was injected into HPLC at 10, 60, 180, 240, and 360 min post-synthesis and analyzed for change in radiochemical purity over time by using the QC HPLC procedure.

Lipophilicity measurement—Lipophilicity of [^{18}F]-DAFBA was determined via the shake flask method using a 1-octanol and phosphate-buffered saline (pH 7.4) system as described by Wilson *et al.* (26). Briefly, ~500 Kcpm of [^{18}F]-DAFBA was added to test tubes containing a 1-octanol (1mL) and PBS (1mL) mixture (in triplicate) and the test-tubes were vortexed for 3 min. Subsequently, the two layers were allowed to separate, aliquots (100μL) of the organic and the aqueous layers were withdrawn from each tube, measured for radioactivity, and the Log P value calculated (26,27).

In Vitro Uptake assay—The cells were grown to 80 – 90% confluence in flasks before trypsinizing, and then were re-suspended in PBS, pH 7.4. After assessing the cell counts, 1×10^5, 5×10^5, 8×10^5, and 1×10^6 cells were aliquoted in triplicates in eppendorf tubes. To each tube, ~ 200 Kcpm of [^{18}F]-DAFBA was added and the tubes were incubated at 22°C (ambient temperature) for 1 hr. After incubation, the tubes were centrifuged, the media was removed, the pellet washed with PBS, and the combined wash and the pellets were counted for radioactivity using a gamma counter. The percent uptake (% uptake) was calculated as the percent of the total added radioactivity found in the pellet.

Sigma receptor binding assay—The IC_{50} values for the binding of DAFBA to sigma receptors were performed by using competitive binding assay. For sigma-1 receptor binding, the assay was performed using the guinea pig brain membrane and the ligand ^{3}H-PENT as described earlier (28). For sigma-2 receptor binding, the assay was performed using rat liver membrane prepared from Sprague-Dawley rats and ligand ^{3}H-DTG in the presence of 1μM dextrallorphane to mask sigma-1 receptors, as described earlier (29). The competition binding assays for both the receptors was performed using 7 concentrations of DAFBA ranging from 10^{-6} to 10^{-9} M. The IC_{50}, and K_i values were calculated using Prism Software (GraphPad software Inc., La Jolla, CA).

Tissue Distribution studies in normal ICR mice—The biodistribution studies were performed using ICR mice. The mice were injected with ~15 μCi of [^{18}F]-DAFBA in 100μL saline via the tail vein injection. At 30, 60, 120, and 180 min post injection, the animals were euthanized, tissues of interest removed, washed with PBS, weighed, and counted for radioactivity using a gamma-counter. The accumulation of radioactivity in various tissues is expressed as percent-injected dose per gram of tissue (%ID/g) by counting the injected dose standard of appropriate count rate along with the tissues. The statistical significance of differences was determined by unpaired Student's t-test using the Microsoft Excel program. Differences were considered significant when $P< 0.05$ was obtained.

Tissue distribution studies using C57 mice bearing B16F1 tumor xenograft— Mouse melanoma cells B16-F1 were grown in DMEM media as described above. When the flasks were 80–90% confluent, the cells were trypsinized, removed from flask, centrifuged, and re-suspended in a 50:50 mixture of Matrigel (Becton Dickinson, San Jose, CA) and PBS (pH 7.4) for inoculation in the animals. The mice were inoculated with 0.1mL cell suspension in PBS-containing ~5×10^6 cells in the right flank with a 23-gauge needle. The tumor growth was monitored periodically. The biodistribution studies were performed when the tumor volume reached >200 mm^3. The tumor bearing mice were injected with of ~15 μCi of [^{18}F]-DAFBA in 100μL saline via the tail vein injections. F-18 uptake in tumor and other tissues was assessed at 30, 60, 120, and 180 min post injection. At preset time points, the animals were euthanized, tissues of interest removed, washed with PBS, weighed and counted for radioactivity using a gamma-counter.

RESULTS AND DISCUSSION

Synthesis of DAFBA, the non-radioactive compound, is shown in Scheme 1. The desired product was obtained in 84% yield and in 98% chemical purity after flash column chromatography. The DAFBA was eluted at 22±1 min using a semi-preparatory HPLC column. On the QC column, this product was eluted at 11.1±0.4 min. This non-radiolabeled DAFBA was prepared as an HPLC reference standard for the production of radioactive compound [^{18}F]-DAFBA. The radiochemical synthesis of [^{18}F]-DAFBA was accomplished using two separate routes and is shown in Scheme 2. For the first method, initially 4-[^{18}F] fluorobenzaldehyde was prepared followed by oxidation of the aldehyde group to carboxylic acid group. Using this route, 4-[^{18}F]Fluorobenzoic acid was synthesized in 72±11 % (n=12) radiochemical yields. Alternatively, the 4-[^{18}F]fluorobenzoic acid **4** was prepared in 82±8% (n=11) radiochemical yields in two steps, first by preparing ethyl [^{18}F]fluorobenzoate followed by hydrolyzing the ester group to yield 4-[^{18}F]fluorobenzoic acid **4** without isolating the intermediate ethyl ester. The coupling of N-*N*-diethylethylenediamine to 4-[^{18}F]fluorobenzoic acid **4** was accomplished using EDC as the coupling agent. After the reaction, the mixture was loaded on semi-prep HPLC column and the desired product was eluted from the column (retention time 22.2 min) in 54±18% radiochemical yields (n=17) and 97 ± 2% radiochemical purity. The purity and the specific activity of this product were determined using the QC HPLC system. The retention time of [^{18}F]-DAFBA on QC-HPLC column was 11.3 min and the specific activity remained >1000 mCi/μmol for all preparations. The overall synthesis time for [^{18}F]-DAFBA including the HPLC purification and the final formulation was 175±15 min (n=17). To assess stability of [^{18}F]-DAFBA over extended period of time, an aliquot of the product was injected on QC-HPLC column at various time points for up to six hours post preparation of the product. The shelf-life stability studies showed radiochemical purity of [^{18}F]-DAFBA remained >95% at all time points demonstrating the stability of the radiotracer over the six hour storage period. While these studies were performed to assess the expiration time for this radioactive compound, this data does not reflect *in vivo* stability of the molecule. While the assessment of bio-stability and metabolic fate of this compound *in vivo* remains outside the scope of this study, these important studies are part of extensive characterization of this compound as imaging probe.

Cell uptake studies were performed using the B16F1 mouse melanoma cells. Triplicate sets of eppendorf tubes containing various concentrations of cells were incubated with [^{18}F]-DAFBA at room temperature for 60 min. The cells were separated, washed and counted for the radioactivity to determine the percentage of added radioactivity taken up by the cells. The cell uptake data is shown in Figures 1. As see in figure 1, the uptake of [^{18}F]-DAFBA increased with increasing number of cells with an uptake of 5.60±2.67% when 1×10^6 cells/tube were incubated with [^{18}F]-DAFBA.

Role of Sigma Receptors

The role of sigma receptors on the tumor cells has been implicated in uptake of radioiodinated benzamides in certain tumors. Although it is not known whether B16F1 cells used in our study express sigma receptors, various other tumor cell lines such as PC12, A375 amelanotic melanoma, T47D breast ductal carcimona, SK-N-SH neuroblastoma, and C6 glioma cells highly express sigma receptors. Since these tumor cell lines also show high binding to iodobenzamides, several investigators hypothesized that binding ability of iodobenzamides to sigma receptors could be exploited to image melanoma and other tumors (30–33). For that reason, John *et al.* synthesized a series of iodobenzamides that showed high sigma receptor binding and displayed varying efficacy to image various tumors (34,35). Therefore, we also evaluated sigma receptor binding of DAFBA *in vitro.* Surprisingly, the *in vitro* binding assay showed a lack of any appreciable binding of DAFBA to sigma-1 and sigma-2 receptors and the IC_{50} for the DAFBA was >1000 nM to both of these receptors. Despite lack of affinity towards sigma receptors, we observed encouraging [^{18}F]-DAFBA uptake results using the B16F1 melanoma cells. A more expanded *in vivo* structure-activity-relationship study performed by Eisenhut *et al.* revealed that the binding of iodinated benzamide to melanoma tumor does not correlate with sigma receptor binding and concluded that sigma receptors are not important for uptake of iodobenzamides by the melanoma tumors and cells (36). Interestingly, an attempt to block sigma receptors *in vivo* by injecting DuP 734 prior to iodobenzamide administration resulted in two-fold increased uptake in the tumor while it significantly reduced its uptake in the brain and the lungs. These findings further demonstrate that uptake in melanoma tumors is independent of sigma receptors (33). The low *in vitro* binding affinity towards sigma-1 and sigma-2 receptors along with a modest *in vitro* cell uptake to B16F1 cells seen for [^{18}F]-DAFBA further support those findings.

To explore *in vivo* tissue distribution characteristics of [^{18}F]-DAFBA, the biodistribution studies were performed using the ICR normal mice. The F-18 uptake in various tissues from that study is summarized in Table 1. In general, a low F-18 uptake was observed in most normal tissues. As expected, at earlier time point (30 min), the uptake in the liver and kidneys was somewhat higher than other normal tissues (liver 3.12±0.62 %ID/g; kidneys 4.13±0.68 %ID/g). Nonetheless, the radioactivity from liver rapidly washed out with time, approaching the levels seen in other normal tissue (liver 1.12±0.20 at 180 min). Similarly, the radioactivity in the blood was quite low at all time points studies with radioactivity levels of 0.20±0.04 %ID/g at 120 min post injection.

Since only a few studies have reported the biodistribution characteristics of iodinated benzamides in normal mice, we could only compare our results to biodistribution results reported for the [*I]*N*-(2-diethylaminoethyl) 3-iodo 4-methoxybenzamide ([*I]IMBA), a closely matched structural analogue, that used the C57 normal mice (37). The radioiodine uptake levels in most tissues reported for [*I]IMBA were similar to F-18 uptake observed in the current study. For example, in the current study at 60 min post injection, the F-18 in the liver, lungs, and blood was 3.12±0.62, 1.75±0.43, and 0.78±0.07 %ID/g, respectively, as compared to 3.09±0.45, 1.06±0.23, and 0.84±0.08 %ID/g, respectively, as reported for the [*I]IMBA (37). The uptake differences in various tissues between the two studies were small and statistically insignificant ($p>0.01$). Although the thyroid uptake data was not reported for the [*I]IMBA, a high uptake in the stomach (9.72±1.51%ID/g) and in intestine (7.70±4.70% ID/g) indicated extensive *in vivo* dehalogenation. In contrast, the [^{18}F]-DAFBA was found to be quite stable *in vivo* as evident from its low F-18 uptake in the bones (60 min: 0.69±0.08 % ID/g) that continued to decrease further with time. Despite a disparate specific activities of the tracers used in these two studies (IMBA 0.1–1.0 mCi/μmole; [^{18}F]DAFBA >1000 mCi/μmole) and varied lipophilicities, the tissue distribution results for the two molecules were fairly similar..

To further characterize [^{18}F]-DAFBA for its tumor uptake properties, the biodistribution studies were performed using C57 mice bearing B16F1 melanoma tumor xenografts. The F-18 uptake in various tissues is shown in Table 2. The F-18 accumulation for the tumor bearing mice was quite similar to that observed using the ICR normal mice. Most normal tissues from tumor bearing mice showed a low accumulation at all time points studied. The radioactivity continued to clear out from normal tissues with time. For example, the F-18 uptake in the muscles was 1.1±0.14 %ID/g at 30 min that was further reduced to 0.17±0.03 %ID/g at 180 min post injection, exhibiting a six-fold reduction. Similarly, the F-18 level in the blood was 0.58±0.18%ID/g and 0.13±0.03 %ID/g at 30 min and 180 min, respectively. A rapid *in vivo* clearance of radioactivity and low levels of circulating radioactivity in the blood pool reflected a low affinity of this compound towards erythrocytes and serum proteins. One of the advantages of this low circulating radioactivity in the blood would be clear visualization of tumor and metastases *in vivo* using this probe. The metabolic tissues such as liver and spleen also showed low uptake of radioactivity that continued to clear out further with time. As seen in normal mice, the bone uptake in tumor mice remained significantly low, thereby underscoring the stability of [^{18}F]-DAFBA towards *in vivo* dehalogenation.

In this study, [^{18}F]-DAFBA displayed a rapid and high uptake in the tumor. The [^{18}F]-DAFBA uptake in B16F1melanoma tumor xenograft is shown in figure 2. The tumor uptake reached to 7.00±2.76 %ID/g by 60 min. While the tumor accumulation decreased slightly by 180 min (5.80 ±0.98%ID/g), the tumor uptake differences between 60 min and 180 min time points were small and statistically insignificant ($p>0.2$).

Earlier, Pham *et al.* suggested that iodobenzamides with higher lipophilicity would show better tumor uptake properties. They further hypothesized that a $logP_{7.4}$ of greater than 1.4 is necessary for the enhanced tumor uptake characteristics (38). Using the Chem-Draw Ultra software (Cambridge Sof.Com, Cambridge, MA), the calculated logP values of for the [*I] IBZA and [^{18}F]-DAFBA were 3.21 and 2.01, respectively. Both of these compounds showed higher than the minimal suggested logP value of 1.4, indicating that they should be useful melanoma imaging agents (38). Since Pham *et al.* suggested lipophilicity of benzamides as one of the important determinants for their biological efficacy, we experimentally measured the partition coefficient of [^{18}F]-DAFBA using the 1-octanol:PBS method described earlier (26). The measured partition co-efficient for [^{18}F]-DAFBA was 1.7, a value similar to its calculated logP value as stated above. It is possible that iodine for fluoride substitution may have resulted in significantly decreased lipophilicity of [^{18}F]-DAFBA. While the lipophilicity remains an important feature for improved tissue membrane penetration, multiple factors play critical role to achieve favorable tracer uptake and kinetics (27,39). A higher lipophilicity (higher logP) may enhance tissue penetration to improve tumor uptake; it simultaneously would increase the non-target tissue uptake and lead to higher non-specific uptake in target and in non-target tissues. Therefore, it is important to carefully balance physico-chemical parameters when designing new probes. In essence, several investigations explicate that the lipophilicity measure of melanoma-specific compounds remains a less reliable predictor of their *in vivo* behavior (27,40). Physiological parameters such as specific activity of radioactive probe, metabolism, clearance, and excretion are some of the other factors that play vital role in defining merits of a potentially useful imaging probe.

In order to assess correlation between the radioactivity levels in the blood and its uptake in the tumor, the blood uptake values (%ID/g) from individual mice were plotted against respective tumor uptake values (%ID/g). The data presented in figure 3 suggest that the tumor uptake is not dependent on the amount of radioactivity present in the blood pool. While the radioactivity levels in the blood decreased significantly by 120 min, the radioactivity levels in the tumor remained unchanged. No correlation was noted between blood and tumor uptake values. The Pearson Coefficient of correlation for these two variables was 0.32.

A high F-18 uptake in tumor and low accumulation of radioactivity in normal tissues resulted in a favorable tumor to tissue ratio for [^{18}F]-DAFBA. The tumor to normal tissue ratios for various tissues is presented in figure 4. The tumor to blood ratio increased from 8.3±3 at 60 min to 39±12 by 180 min, a five-fold increase. Similarly, tumor to lung and tumor to muscle ratios for [^{18}F]-DAFBA were >20 at 180 min. Except for the kidneys, the tumor to tissue ratio for most tissues remained high at 180 min. These results were quite similar to that reported by Moins *et al* using the [*I]IBZA(27). A rapid and high tumor uptake along with a high tumor to normal-tissue ratios seen herein are exceedingly significant because it underscores the potential of this compound for aiding in clear visualization of tumors and its metastases non-invasively and within a time frame compatible with the PET isotope half-life.

The brain is one of the common sites that develop melanoma metastases. Therefore, we were interested in exploring whether [^{18}F]-DAFBA enters the brain by crossing the blood-brain barrier. The tissue distribution studies performed in normal and tumor-bearing mice showed [^{18}F]-DAFBA enters in the brain within 30 min. At early time points, the radioactivity levels were 2-fild higher in the brain than in other normal organs. After initial high uptake, the radioactivity continued to clear from the brain with time. For example, the F-18 uptake in the brain was 2.02±0.35 %ID/g at 30 min and reduced to one-tenth of this value by 180 min. While initial accumulation in the brain showed its ability to enter the brain, a rapid washout displayed a low affinity of [^{18}F]-DAFBA towards non-tumoral tissues, a positive attribute for a potentially useful imaging agent. [^{18}F]-DAFBA also showed encouraging uptake characteristics in the lungs and the liver, two other tissues known to anchor melanoma metastases. As evident from data presented in Table 2, the uptake and clearance of [^{18}F]-DAFBA in the lungs is similar to that seen for the brain. At 30 min, the F-18 uptake in the lungs was slightly higher than that in the brain, it decreased exponentially with time and reached radioactivity levels similar to that in the blood by 180 min. The initial modest uptake following a rapid elimination of radioactivity from the organs of metastatic potential would constitute a positive trait for this probe. If developed further, this probe may have significant potential in delineating brain and lung metastases from normal tissue.

Two of the major traits for a successful imaging agent are high uptake of radioactivity in the tumor and low retention of radioactivity in normal tissues. In the current study, [^{18}F]-DAFBA exhibits both of these properties. A high uptake and retention of radioactivity in tumor at 60 min along with low retention of radioactivity in normal tissues suggests that if developed further, [^{18}F]-DAFBA could be potentially useful PET imaging probe to image melanoma.

In summary, we successfully synthesized a melanoma-seeking PET imaging agent [^{18}F]-DAFBA. The radiochemical synthesis was achieved in high radiochemical yields and in a synthesis time compatible with F-18 half-life. The *in vitro* studies showed that [^{18}F]-DAFBA binds to the melanoma cells. Biodistribution studies in mice showed a rapid and high uptake in the tumor and a low accumulation of F-18 in normal tissues pointing to its potential to provide a high signal to noise ratio and to its ability to clearly visualize tumors with low background signals. Besides, a low bone uptake signifies the stability of this ligand towards *in vivo* dehalogenation. Based on these promising *in vitro* and *in vivo* results, it is tempting to envision the potential of [^{18}F]-DAFBA as a useful melanoma imaging agent using PET. Additional studies are necessary to fully explore the potential of [^{18}F]-DAFBA as a melanoma imaging agent using PET.

Acknowledgments

We would like to thank Kimberly Black, Holly Smith, and Li Wu for their excellent technical help with the cell uptake assay and tissue distribution studies. We also thank the cyclotron staff for their help with radioisotope production. The partial financial support for this study from NIH (CA 105383 to PKG) is greatly appreciated.

LITERATURE CITED

1. Chen J, Giblin MF, Wang N, Jurisson SS, Quinn TP. In vivo evaluation of 99mTc/188Re-labeled linear alpha-melanocyte stimulating hormone analogs for specific melanoma targeting. Nucl Med Biol 1999;26:687–693. [PubMed: 10587108]
2. Buraggi GL, Callegaro L, Mariani G, Turrin A, Cascinelli N, Attili A, Bombardieri E, Terno G, Plassio G, Dovis M, et al. Imaging with 131I-labeled monoclonal antibodies to a high-molecular-weight melanoma-associated antigen in patients with melanoma: efficacy of whole immunoglobulin and its F(ab')2 fragments. Cancer Res 1985;45:3378–3387. [PubMed: 4005860]
3. Garg PK, Alston KL, Welsh PC, Zalutsky MR. Enhanced binding and inertness to dehalogenation of alpha-melanotropic peptides labeled using N-succinimidyl 3-iodobenzoate. Bioconj Chem 1996;7:233–239.
4. Miao Y, Quinn TP. Peptide-targeted radionuclide therapy for melanoma. Crit Rev Oncol Hematol 2008;67:213–228. [PubMed: 18387816]
5. Boyd CM, Lieberman LM, Beierwaltes WH, Varma VM. Diagnostic efficacy of a radioiodinated chloroquine analog in patients with malignant melanoma. J Nucl Med 1970;11:479–486. [PubMed: 4916113]
6. Lambrecht RM, Packer S, Wolf AP, Lloyd D, Atkins HL. Detection of ocular melanoma with 4-(3-dimethylaminopropylamino)-7-[123I]-iodoquinoline. J Nucl Med 1984;25:800–804. [PubMed: 6737079]
7. Ono S, Fukunaga M, Otsuka N, Nagai K, Morita K, Furukawa T, Muranaka A, Yanagimoto S, Tomomitsu T, Tabuchi A, et al. Visualization of ocular melanoma with N-isopropyl-p-[123I]-iodoamphetamine. J Nucl Med 1988;29:1448–1450. [PubMed: 3404259]
8. Cohen MB, Saxton RE, Lake RR, Cagle L, Graham LS, Nizze A, Yamada LS, Gan M, Bronca G, Greenwell K, et al. Detection of malignant melanoma with iodine-123 iodoamphetamine. J Nucl Med 1988;29:1200–1206. [PubMed: 3392580]
9. Osei-Bonsu A, Kokoschka EM, Ulrich W, Sinzinger H. 131I-metaiodobenzylguanidine (mIBG) for bronchial oat cell cancer and melanoma detection? Eur J Nucl Med 1989;15:629–631. [PubMed: 2557215]
10. Michelot JM, Moreau MF, Veyre AJ, Bonafous JF, Bacin FJ, Madelmont JC, Bussiere F, Souteyrand PA, Mauclaire LP, Chossat FM, et al. Phase II scintigraphic clinical trial of malignant melanoma and metastases with iodine-123-N-(2-diethylaminoethyl 4-iodobenzamide). J Nucl Med 1993;34:1260–1266. [PubMed: 8326382]
11. Moins N, D'Incan M, Bonafous J, Bacin F, Labarre P, Moreau MF, Mestas D, Noirault E, Chossat F, Berthommier E, Papon J, Bayle M, Souteyrand P, Madelmont JC, Veyre A. 123I-N- (2-diethylaminoethyl)-2-iodobenzamide: a potential imaging agent for cutaneous melanoma staging. Eur J Nucl Med Mol Imaging 2002;29:1478–1484. [PubMed: 12397467]
12. Brenner W, Klomp HJ, Bohuslavizki KH, Szonn B, Kampen WU, Henze E. Limited sensitivity of iodine-123-2-hydroxy-3-iodo-6-methoxy-N-[(1-ethyl-2-pyrrolidinyl)methyl] benzamide whole-body scintigraphy in patients with malignant melanoma: a comparison with thallium-201 imaging. Eur J Nucl Med 1999;26:1567–1571. [PubMed: 10638408]
13. Maffioli L, Mascheroni L, Mongioj V, Gasparini M, Baldini MT, Seregni E, Castellani MR, Cascinelli N, Buraggi GL. Scintigraphic detection of melanoma metastases with a radiolabeled benzamide ([iodine-123]-(S)-IBZM). J Nucl Med 1994;35:1741–1747. [PubMed: 7965150]
14. Wagner JD, Schauwecker D, Davidson D, Logan T, Coleman JJ 3rd, Hutchins G, Love C, Wenck S, Daggy J. Inefficacy of F-18 fluorodeoxy-D-glucose-positron emission tomography scans for initial evaluation in early-stage cutaneous melanoma. Cancer 2005;104:570–579. [PubMed: 15977211]
15. Wagner JD. A role for FDG-PET in the surgical management of stage IV melanoma. Ann Surg Oncol 2004;11:721–722. [PubMed: 15249339]
16. Acland KM, Healy C, Calonje E, O'Doherty M, Nunan T, Page C, Higgins E, Russell-Jones R. Comparison of positron emission tomography scanning and sentinel node biopsy in the detection of micrometastases of primary cutaneous malignant melanoma. J Clin Oncol 2001;19:2674–2678. [PubMed: 11352959]

17. Hafner J, Schmid MH, Kempf W, Burg G, Kunzi W, Meuli-Simmen C, Neff P, Meyer V, Mihic D, Garzoli E, Jungius KP, Seifert B, Dummer R, Steinert H. Baseline staging in cutaneous malignant melanoma. Br J Dermatol 2004;150:677–686. [PubMed: 15099363]
18. Michelot JM, Moreau MF, Labarre PG, Madelmont JC, Veyre AJ, Papon JM, Parry DF, Bonafous JF, Boire JY, Desplanches GG, et al. Synthesis and evaluation of new iodine-125 radiopharmaceuticals as potential tracers for malignant melanoma. J Nucl Med 1991;32:1573–1580. [PubMed: 1869982]
19. Brandau W, Kirchner B, Bartenstein P, Sciuk J, Kamanabrou D, Schober O. N-(2-diethylaminoethyl)-4-[123I]iodobenzamide as a tracer for the detection of malignant melanoma: simple synthesis, improved labelling technique and first clinical results. Eur J Nucl Med 1993;20:238–243. [PubMed: 8462613]
20. Mansard S, Papon J, Moreau MF, Miot-Noirault E, Labarre P, Bayle M, Veyre A, Madelmont JC, Moins N. Uptake in melanoma cells of N-(2-diethylaminoethyl)-2-iodobenzamide (BZA2), an imaging agent for melanoma staging: relation to pigmentation. Nucl Med Biol 2005;32:451–458. [PubMed: 15982575]
21. Sillaire-Houtmann I, Bonafous J, Veyre A, Mestas D, D'Incan M, Moins N, Kemeny JL, Chossat F, Bacin F. [Phase 2 clinical study of 123I-N-(2-diethylaminoethyl)-2-iodobenzamide in the diagnostic of primary and metastatic ocular melanoma]. J Fr Ophtalmol 2004;27:34–39. [PubMed: 14968075]
22. Wilson AA, Dannals RF, Ravert HT, Wagner HN. Reductive Amination of [18F] fluorobenzaldehydes: Radiosynthesis of 2-[18F] and 4-[18F]fluorodexetimides. J Labelled Comp Radiopharm 1990;XXXVIII:1189–1199.
23. Garg PK, Garg S, Zalutsky MR. Synthesis and preliminary evaluation of *para*- and *meta*- [^{18}F] fluorobenzylguanidine. Nuc Med Biol 1994;21:97–103.
24. Haka MS, Kilbourn MR, Watkins GL, Torongian S. Arylmethylammonium trifluoromethanesulfonates as precursors to aryl [F-18]fluorides: Improved synthesis of [F-18] GBR-13119. J Label Compound Radiopharm 1989;27:823–833.
25. Marik J, Sutcliffe JL. Fully automated preparation of n.c.a. 4-[18F]fluorobenzoic acid and N-succinimidyl 4-[18F]fluorobenzoate using a Siemens/CTI chemistry process control unit (CPCU). Appl Radiat Isot 2007;65:199–203. [PubMed: 16935516]
26. Wilson AA, Jin L, Garcia A, DaSilva JN, Houle S. An admonition when measuring the lipophilicity of radiotracers using counting techniques. Appl Radiat Isotopes 2001;54:203–208.
27. Moins N, Papon J, Seguin H, Gardette D, Moreau MF, Labarre P, Bayle M, Michelot J, Gramain JC, Madelmont JC, Veyre A. Synthesis, characterization and comparative biodistribution study of a new series of p-iodine-125 benzamides as potential melanoma imaging agents. Nucl Med Biol 2001;28:799–808. [PubMed: 11578901]
28. Bowen WD, de Costa BR, Hellewell SB, JM W, Rice KC. [^{3}H]-(+)-Pentazocine: a potent and highly selective benzomorphane based probe for sigma-1 receptors. Mol Neuropharmacol 1993;3:117– 126.
29. Hellewell SB, Bruce A, Feinstein G, Orringer J, Williams W, Bowen WD. Rat liver and kidney contain high densities of sigma 1 and sigma 2 receptors: characterization by ligand binding and photoaffinity labeling. Eur J Pharmacol 1994;268:9–18. [PubMed: 7925616]
30. John CS, Vilner BJ, Gulden ME, Efange SM, Langason RB, Moody TW, Bowen WD. Synthesis and pharmacological characterization of 4-[125I]-N-(N-benzylpiperidin-4-yl)-4-iodobenzamide: a high affinity sigma receptor ligand for potential imaging of breast cancer. Cancer Res 1995;55:3022–3027. [PubMed: 7606722]
31. Staelens L, Oltenfreiter R, Dumont F, Waterhouse RN, Vandenbulcke K, Blanckaert P, Dierckx RA, Slegers G. In vivo evaluation of [123I]-4-iodo-N-(4-(4-(2-methoxyphenyl)-piperazin-1-yl)butyl)-benzamide: a potential sigma receptor ligand for SPECT studies. Nucl Med Biol 2005;32:193–200. [PubMed: 15721765]
32. Vilner BJ, John CS, Bowen WD. Sigma-1 and sigma-2 receptors are expressed in a wide variety of human and rodent tumor cell lines. Cancer Res 1995;55:408–413. [PubMed: 7812973]
33. Waterhouse RN, Chapman J, Izard B, Donald A, Belbin K, Obrien JC, Collier TL. Examination of four ^{123}I labeled piperidine-based sigma receptor ligands as potential melanoma imaging agents—initial studies in mouse tumor models. Nucl Med Biol 1997;24:587–593. [PubMed: 9316089]

34. John CS, Bowen WD, Saga T, Kinuya S, Vilner BJ, Baumgold J, Paik CH, Reba RC, Neumann RD, Varma VM, et al. A malignant melanoma imaging agent: synthesis, characterization, in vitro binding and biodistribution of iodine-125-(2-piperidinylaminoethyl)4-iodobenzamide. J Nucl Med 1993;34:2169–2175. [PubMed: 8254405]

35. John CS, Vilner BJ, Bowen WD. Synthesis and characterization of [^{125}I]-*N*-(*N*-benzylpiperidin- 4-yl)-4-iodobenzamide, a new sigma receptor radiopharmaceutical: high affinity binding to MCF- 7 breast tumor cells. J Med Chem 1994;37:1737–1739. [PubMed: 8021913]

36. Eisenhut M, Hull WE, Mohammed A, Mier W, Lay D, Just W, Gorgas K, Lehmann WD, Haberkorn U. Radioiodinated N-(2-diethylaminoethyl)benzamide derivatives with high melanoma uptake: structure-affinity relationships, metabolic fate, and intracellular localization. J Med Chem 2000;43:3913–3922. [PubMed: 11052796]

37. Edreira MM, Pozzi OR. Iodide benzamides for the in-vivo detection of melanoma and metastases. Melanoma Res 2006;16:37–43. [PubMed: 16432454]

38. Pham TQ, Greguric I, Liu X, Berghofer P, Ballantyne P, Chapman J, Mattner F, Dikic B, Jackson T, Loc'h C, Katsifis A. Synthesis and evaluation of novel radioiodinated benzamides for malignant melanoma. J Med Chem 2007;50:3561–3572. [PubMed: 17602544]

39. Brandau W, Niehoff T, Pulawski P, Jonas M, Dutschka K, Sciuk J, Coenen HH, Schober O. Structure distribution relationship of iodine-123-iodobenzamides as tracers for the detection of melanotic melanoma. J Nucl Med 1996;37:1865–1871. [PubMed: 8917194]

40. Nicholl C, Mohammed A, Hull WE, Bubeck B, Eisenhut M. Pharmacokinetics of iodine- 123-IMBA for melanoma imaging. J Nucl Med 1997;38:127–133. [PubMed: 8998166]

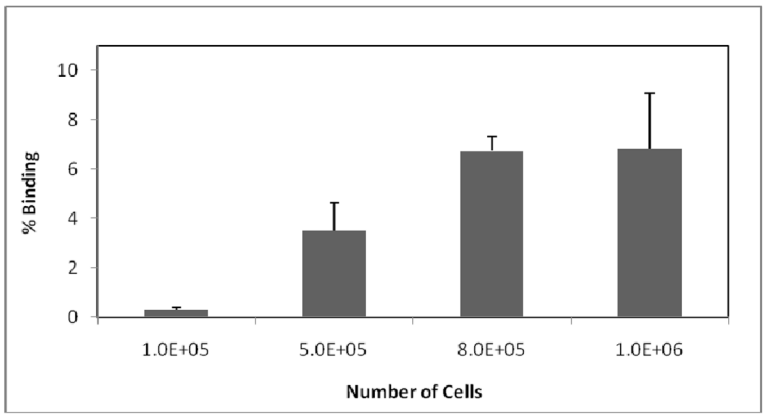

Figure 1.

In vitro binding of [^{18}F]-DAFBA to B16F1 melanoma cells. Various concentrations of cells were incubated with [^{18}F]-DAFBA for 60 min at room temperature. The results are presented as a percent of total added radioactivity that was taken up by the cells (mean ± standard deviation; n= 3 tubes for each concentration).

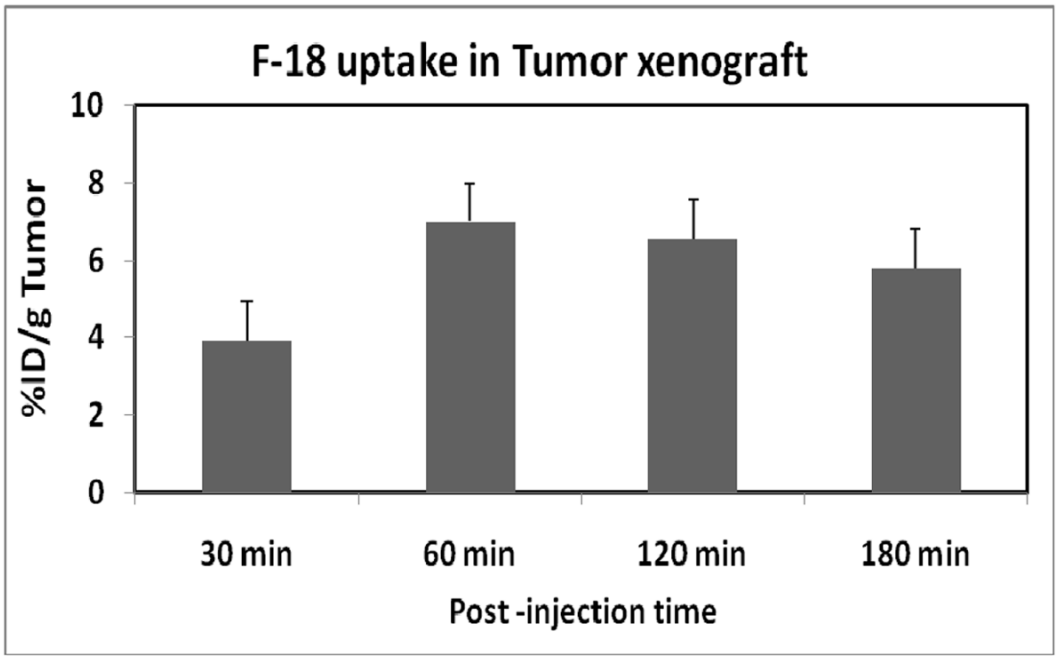

Figure 2.
F-18 uptake in the tumor at 30, 60, 120, and 180 min post injection of [^{18}F]-DAFBA using C57 mice bearing B16F1 melanoma tumor. The data is expressed as percent injected dose per gram of tumor (%ID/g average ± Standard deviation; n=5).

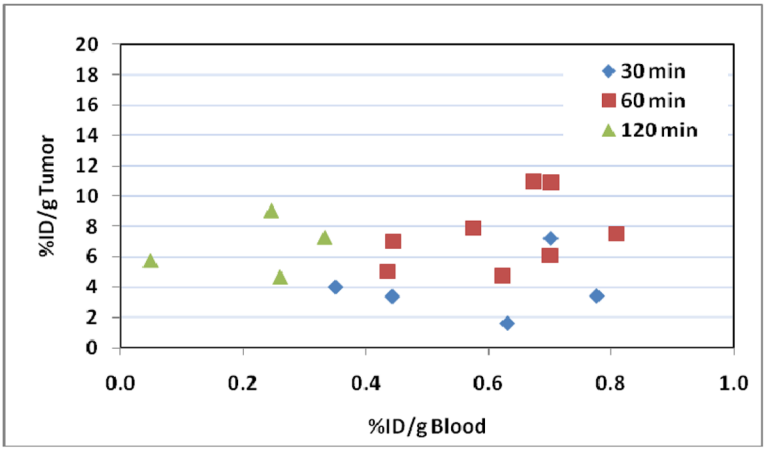

Figure 3.

Correlation plot for [^{18}F]-DAFBA uptake in the melanoma tumor versus the radioactivity present in the blood at 30, 60, and 120 min. Each data point represents data from a single mouse. The plot shows the radioactivity levels in the blood pool is independent of radioactivity in the tumor and the two variables exhibit a poor Pearson correlation (r=0.398).

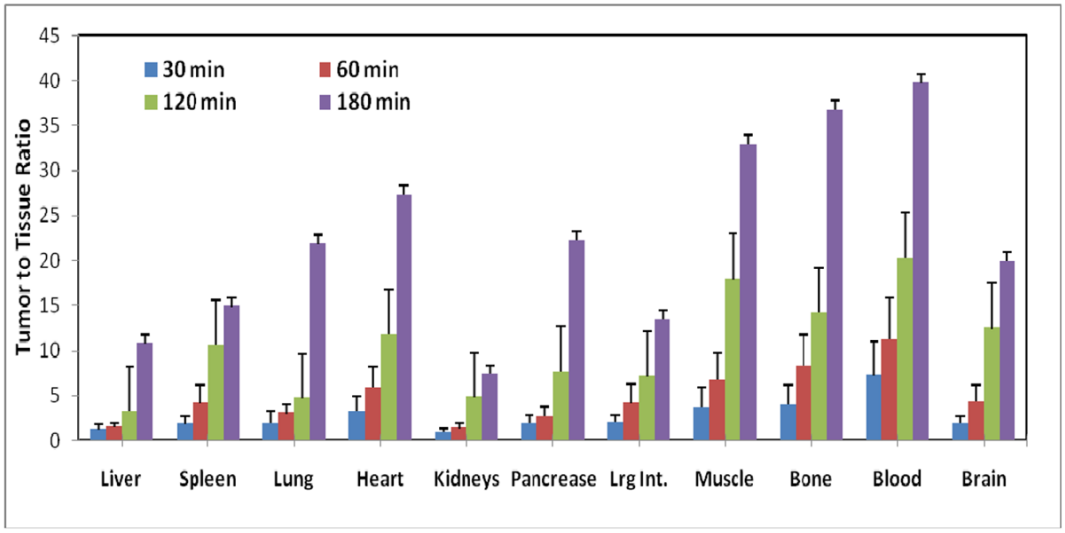

Figure 4.

Tumor to normal tissue ratios of [^{18}F]-DAFBA using C57 mice bearing B16F1 melanoma tumor at 30, 60, 120, and 180 min post injection. While modest tumor to normal tissue ratios was observed at 30 min, these ratios continued to improve significantly with time.

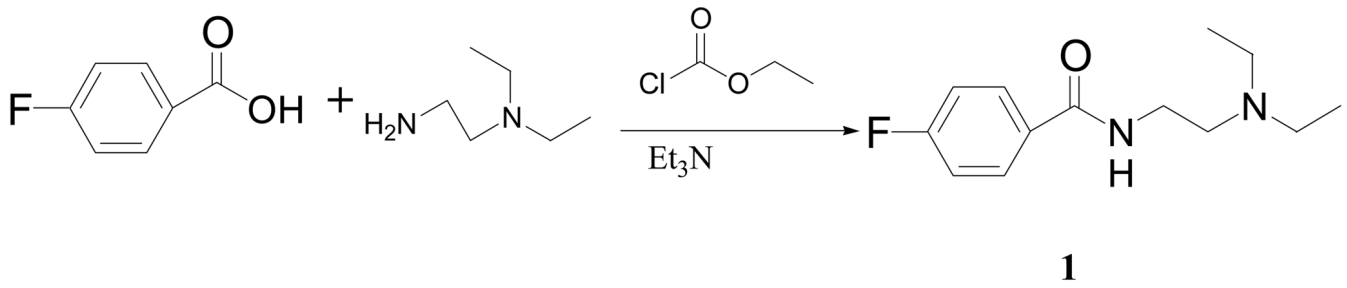

1

Scheme 1.
Reaction scheme for the synthesis of *N*-(2-diethylamino ethyl) 4-fluorobenzamide (DAFBA; **1**).

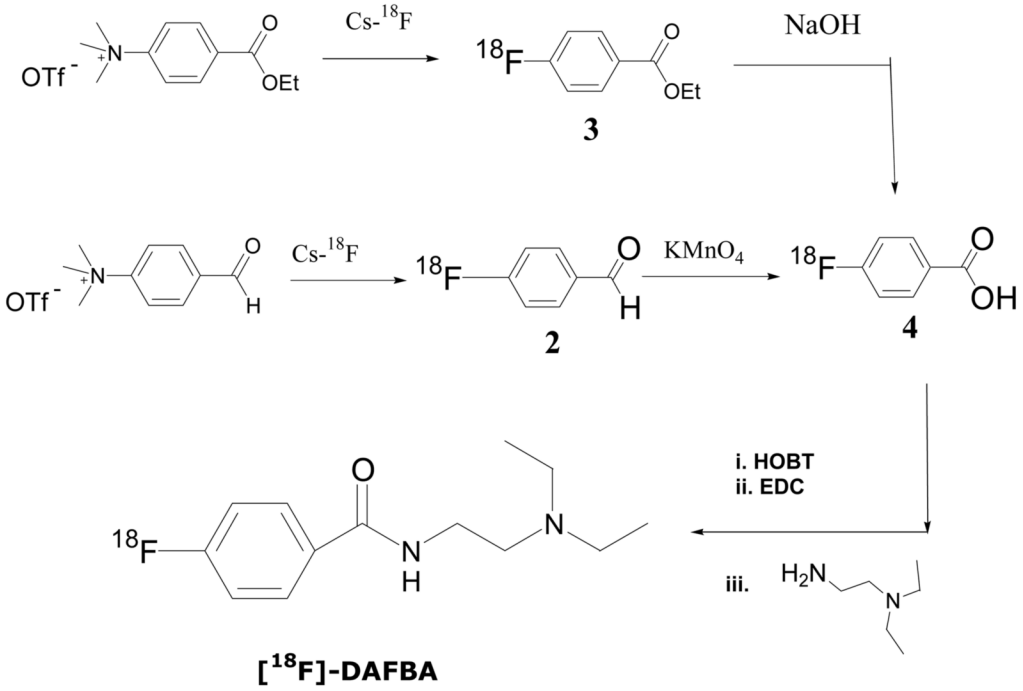

Scheme 2.

Reaction scheme for the preparation of radiolabeled compound *N*-(2-diethylaminoethyl) 4-[^{18}F]fluorobenzamide ([^{18}F]-DAFBA) using 4-[^{18}F]fluorobenzoic acid (**4**) as the intermediate. The compound **4** was prepared utilizing either 4-[^{18}F]fluorobenzaldehyde (**2**) or ethyl 4-[^{18}F] fluorobenzoate (**3**). Subsequent coupling of **4** with *N*-*N*-diethylethylenediamine in the presence of 1-hydroxybenzotriazole hydrate (HOBT) and 1-(3-dimethylaminopropyl)-3-ethylcarbodiimide hydrochloride (EDC) provided the desired compound.

Table 1

Biodistribution of *N*-(2-diethylaminoethyl) 4-[^{18}F]fluorobenzamide ([^{18}F]-DAFBA) in normal Balb/c ICR mice at various time points after injection (mean±SEM; n=5)

	Percent Injected Dose per gram Tissue (%ID/g)			
ORGAN	**30 Min**	**60 Min**	**120 Min**	**180 Min**
Liver	3.12 ± 0.62	3.61 ± 0.48	1.14 ± 0.41	1.12 ± 0.20
Spleen	2.35 ± 0.07	1.87 ± 0.46	0.43 ± 0.25	0.53 ± 0.08
Lung	1.75 ± 0.43	1.84 ± 0.41	0.42 ± 0.14	0.49 ± 0.07
Heart	1.10 ± 0.14	0.92 ± 0.10	0.28 ± 0.05	0.23 ± 0.03
Kidneys	4.13 ± 0.68	4.20 ± 0.41	1.58 ± 0.51	1.34 ± 0.36
Intestine	0.91 ± 0.32	1.39 ± 0.54	0.26 ± 0.26	0.40 ± 0.11
Muscle	0.88 ± 0.13	0.65 ± 0.11	0.18 ± 0.10	0.16 ± 0.03
Bone	0.81 ± 0.19	0.69 ± 0.08	0.20 ± 0.06	0.24 ± 0.10
Blood	0.78 ± 0.07	0.67 ± 0.05	0.20 ± 0.04	0.21 ± 0.03
Brain	2.16 ± 0.32	1.54 ± 0.24	0.52 ± 0.07	0.46 ± 0.07

Table 2

Biodistribution of *N*-(2-diethylaminoethyl) 4-[^{18}F]fluorobenzamide ([^{18}F]-DAFBA) in C57 mice bearing B16F1 melanoma tumor xenograft at various time points after injection (mean±SEM; n=5)

	Percent Injected Dose per gram Tissue (%ID/g)			
ORGAN	**30 Min**	**60 Min**	**120 Min**	**180 Min**
Liver	3.27 ± 0.90	5.01 ± 2.06	2.35 ± 1.20	0.80 ± 0.35
Spleen	2.14 ± 0.41	1.83 ± 0.54	0.71 ± 0.37	0.44 ± 0.25
Lung	2.46 ± 1.27	2.48 ± 1.27	1.47 ± 0.47	0.27 ± 0.07
Heart	1.25 ± 0.28	1.27 ± 0.50	0.61 ± 0.20	0.21 ± 0.04
Kidneys	4.50 ± 1.33	5.38 ± 1.86	1.41 ± 0.11	0.83 ± 0.23
Intestine	1.94 ± 0.51	1.98 ± 0.88	1.02 ± 0.33	0.46 ± 0.22
Muscle	1.09 ± 0.18	1.10 ± 0.38	0.57 ± 0.54	0.17 ± 0.03
Bone	1.00 ± 0.14	0.90 ± 0.27	0.57 ± 0.32	0.17 ± 0.05
Blood	0.58 ± 0.18	0.68 ± 0.21	0.43 ± 0.47	0.13 ± 0.03
Brain	2.02 ± 0.35	1.68 ± 0.43	0.64 ± 0.40	0.29 ± 0.05